






Article

Mathematical Model of Pancreatic Cancer Cell Dynamics Considering the Set of Sequential Mutations and Interaction with the Immune System

Alexander S. Bratus ^{1,2,*} , Nicholas Leslie ³ , Michail Chamo ¹, Dmitry Grebennikov ^{4,5,6} ,
Rostislav Savinkov ^{4,5,7}, Gennady Bocharov ^{4,5,7}  and Daniil Yurchenko ⁸ 

- ¹ Institute of Management and Digital Technologies, Russian University of Transport, 127055 Moscow, Russia
 - ² Moscow Center for Fundamental and Applied Mathematics, Lomonosov Moscow State University, 119991 Moscow, Russia
 - ³ School of Engineering & Physical Sciences, Heriot-Watt University, Edinburgh EH14 4AS, UK
 - ⁴ Marchuk Institute of Numerical Mathematics, Russian Academy of Sciences (INM RAS), 119333 Moscow, Russia
 - ⁵ Moscow Center for Fundamental and Applied Mathematics at INM RAS, 119333 Moscow, Russia
 - ⁶ World-Class Research Center “Digital Biodesign and Personalized Healthcare”, Sechenov First Moscow State Medical University, 119048 Moscow, Russia
 - ⁷ Institute of Computer Science and Mathematical Modeling, Sechenov First Moscow State Medical University, 119048 Moscow, Russia
 - ⁸ Institute for Sound and Vibration Research, University of Southampton, Highfield, Southampton SO17 1BJ, UK
- * Correspondence: alexander.bratus@yandex.ru or bratus@edu.rut-miit.ru



Citation: Bratus, A.S.; Leslie, N.; Chamo, M.; Grebennikov, D.; Savinkov, R.; Bocharov, G.; Yurchenko, D. Mathematical Model of Pancreatic Cancer Cell Dynamics Considering the Set of Sequential Mutations and Interaction with the Immune System. *Mathematics* **2022**, *10*, 3557. <https://doi.org/10.3390/math10193557>

Academic Editor: Dumitru Baleanu

Received: 30 August 2022

Accepted: 26 September 2022

Published: 29 September 2022

Publisher’s Note: MDPI stays neutral with regard to jurisdictional claims in published maps and institutional affiliations.



Copyright: © 2022 by the authors. Licensee MDPI, Basel, Switzerland. This article is an open access article distributed under the terms and conditions of the Creative Commons Attribution (CC BY) license (<https://creativecommons.org/licenses/by/4.0/>).

Abstract: Pancreatic cancer represents one of the difficult problems of contemporary medicine. The development of the illness evolves very slowly, happens in a specific place (stroma), and manifests clinically close to a final stage. Another feature of this pathology is a coexistence (symbiotic) effect between cancer cells and normal cells inside stroma. All these aspects make it difficult to understand the pathogenesis of pancreatic cancer and develop a proper therapy. The emergence of pancreatic pre-cancer and cancer cells represents a branching stochastic process engaging populations of 64 cells differing in the number of acquired mutations. In this study, we formulate and calibrate the mathematical model of pancreatic cancer using the quasispecies framework. The mathematical model incorporates the mutation matrix, fitness landscape matrix, and the death rates. Each element of the mutation matrix presents the probability of appearing as a specific mutation in the branching sequence of cells representing the accumulation of mutations. The model incorporates the cancer cell elimination by effect CD8 T cells (CTL). The down-regulation of the effector function of CTLs and exhaustion are parameterized. The symbiotic effect of coexistence of normal and cancer cells is considered. The computational predictions obtained with the model are consistent with empirical data. The modeling approach can be used to investigate other types of cancers and examine various treatment procedures.

Keywords: pancreatic cancer; cancer evolution; tumor microenvironment; mathematical model; open quasispecies model

MSC: 92-10

1. Introduction

Pancreatic cancer has the worst prognosis of all major cancer types, with very poor treatment options. Less than 10% of patients will live for more than five years after diagnosis [1,2]. The main reasons for this are as follows.

1. The process of formation of precancerous and cancerous cells represents a successive chain of mutations over a relatively long period of time (10 to 20 years). During this time, the disease often causes very limited noticeable symptoms, and the cancer has often already spread at the time of diagnosis, with the most common sites of metastasis being the liver, lung, and peritoneum [3].
2. Pancreatic tumors comprise cancer cells surrounded by other cell types and extracellular matrix, collectively known as the tumor stroma. The dense stroma of pancreatic cancer makes both diagnosis and treatment more difficult [4,5].
3. A favorable microenvironment for tumor progression exists inside the stroma, built in large part upon symbiotic interactions between non-cancerous pancreatic cells and precancerous and cancerous cells [4,6–9].
4. The genetic changes that drive pancreatic cancer do not reveal any clear vulnerabilities to available therapies, and the success with existing treatments is very limited [1,10].

Surgery before the disease has spread remains the only treatment likely to be curative; however, <15% of patients are selected for surgery, and there are no broadly used methods for identifying patients at this early, potentially curable, stage. The most common treatment for metastatic or locally advanced pancreatic cancer are aggressive chemotherapies that modestly extend survival and, to date, targeted therapies have provided little or no benefit [1]. Approximately 85% of pancreatic cancers are defined as pancreatic ductal adenocarcinoma (PDAC), and many, perhaps most, of these tumors are believed to develop from precursor lesions termed pancreatic intraepithelial neoplasia (PanIN) [11]. However, the sequences of genetic changes that lead to PDAC and the consequences of these evolutionary processes on the responses to therapy remain unclear [12,13]. Initial models proposed sequential events in key drivers over many years: activating mutation of a copy of KRAS, followed by bi-allelic loss of CDKN2A, TP53, and SMAD4 [14]. However, more recent data imply that multiple loss of function events may occur simultaneously [15].

Therefore, to deepen our understanding of these processes and to derive testable predictions, we elected to develop a mathematical model of PDAC progression. This describes the dynamics of species communities, taking mutations into account: M. Eigen’s replicator system of quasispecies [16].

Framework for Quasispecies Dynamics

In this study, the quasispecies term implies the set of distinct cell populations (species) that differ with respect to the acquired genetic mutations. The respective mathematical model represents an ODE system describing the evolution of population frequencies, taking into account the set of possible mutations:

$$\frac{dp(t)}{dt} = (QM)p(t) - p(t)f(p) \tag{1}$$

where $p = (p_1, p_2, \dots, p_n)$ is a vector of frequencies (relative numbers of species). Note that in the classical theory of quasispecies, the total number of species remains constant at $t \geq 0$. Matrix $Q = (q_{ij})$, $i, j = 1, 2, \dots, n$ represent the probability of mutations, i.e., q_{ij} sets the probabilities that replicating a species with index j results in a species with number i :

$$\sum_{i=1}^n q_{ij} = 1, \quad j = 1, 2, \dots, n \tag{2}$$

The diagonal matrix $M = \text{diag}(m_1, m_2, \dots, m_n)$ defines the viral fitness landscape. In other words, each species is assigned a number that characterizes its ability to survive in the system. Usually the fitness landscape is quantified on the basis of species growth rates and other data on the dominant properties of the species. The system of quasispecies dynamics describes the evolution of species communities, taking into account possible mutations, but ignoring the natural mortality rates of species. In order to account for species mortality, a modified (open) quasispecies system [16] was proposed, in which the

total number of species is not a constant value. Let $u_i(t)$ be the abundance of species i , $t \geq 0$, M and Q the species adaptation matrix and mutation matrix, respectively.

Let us introduce the following function:

$$S(u) = \sum_{i=1}^n u_i(t) = 1. \tag{3}$$

The function $S(u)$ defines the total number of species at time $t \geq 0$. The function $\Phi(s)$ is characterized by the following properties:

- (a) $\Phi(s)$ is a smooth function $s \in [0, c)$, $c \geq 0$;
- (b) $\Phi(s) > 0$, $s \in [0, c)$;
- (c) If $0 < c < +\infty$, then $\lim_{s \rightarrow c} s\Phi(s) = 0$;
- (d) Function $s\Phi(s) = 0$ has only one maximum at the point s^* , $0 < c < c^*$.

As an example of function $\Phi(s)$, we can consider the functions $\Phi(s) = (c - s)$, $c > 0$, $0 < s < c$, or $\Phi(s) = \exp(-\gamma s)$, $\gamma > 0$, $s > 0$.

Consider the diagonal matrix describing species mortality rates $D = \text{diag}(d_1, d_2, \dots, d_n)$. Let the elements of the fitness landscape matrix M and the mortality matrix satisfy the following conditions:

$$\begin{aligned} 0 &\leq m_{\min} \leq m_i \leq m_{\max} \\ 0 &\leq d_{\min} \leq d_i \leq d_{\max}, \quad i = 1, 2, \dots, n \\ 0 &< d_{\max} < m_{\min}. \end{aligned} \tag{4}$$

Here are the model equations describing the population dynamics of species:

$$\begin{aligned} \frac{du(t)}{dt} &= \Phi(s)(QM)u(t) - Du(t) \\ u(0) &= u^0 \geq 0 \end{aligned} \tag{5}$$

System (5) is positively invariant for any non-negative initial conditions $u(0) \geq 0$. There exists a unique solution to this problem. When conditions in (4) are satisfied, the total number of species (3) as well as the species abundances are bounded functions on the system trajectories [16]. The average fitness of open system (5) is defined by

$$f(u) = \begin{cases} 0, & s(u) = 0 \\ \frac{\sum_{i=1}^n m_i u_i(t)}{\sum_{i=1}^n d_i u_i(t)} = (\Phi(s))^{-1}, & s(u) \neq 0 \end{cases} \tag{6}$$

where the numerator of the expression is equal to the average fitness of quasispecies (1), and the denominator reflects the decline of the species community due to their mortality. Note that the proposed method for describing cell dynamics does not take into account the spatial distribution of cells, which, as a rule, leads to equations of the “reaction-diffusion” type. In the case of the classical Eigen system, it has been proved [17] that the solutions of the “reaction-diffusion” system have the property of diffusion stability with respect to additive additions of diffusion terms. The case of an open replicator system requires a separate study, which is beyond the scope of our research. In this case, to solve the problem, it is possible to use the methods of traveling waves [18–20].

In Section 2, the mutational pathways of the normal cells are characterized. In Section 3, the mathematical model of tumor-immune cell dynamics is developed. The results of numerical simulations are presented in Section 4. The results are briefly discussed in the Conclusions section.

2. Development of the Cancer Mutations

The vast majority (>85%) of pancreatic cancers, defined as pancreatic ductal adenocarcinomas, are driven by activating mutations in a single copy of the KRAS gene (85–95%) and also display very frequent loss of function mutations in TP53 (>75%), CDKN2A (>30–

60%), and SMAD4 (30–50%). Here, these mutations have been abbreviated as K, P, C, and S mutations, respectively. Figure 1 represents the chain of successive mutations of growing pancreatic cancer cell populations. Healthy cells (N) with the potential for oncogenic transformation to PDAC [21,22] are characterized by a high probability of slow error-free replication $p_0 = 0.999999$. Each healthy originating cell can proliferate or die, according to data presented in Table 1, whereas at any given time most of them are non-replicative. Table 1 summarizes the doubling time data for different cell types as well as data on type mortality rates.

Table 1. Data on doubling times and mortality rates for cell types bearing specific mutations.

Mutation Type	Doubling Time (Days)	Mortality
K (KRAS)	200	3.22%
P (TP53)	800	0.86%
C (CDKN2A)	800	1%
S (SMAD4)	900	0.9%
KC	140	15%
KS	180	20%
KP	180	8%
PS	750	5%
CP	600	5%
CS	600	5%
KCS	120	20%
KPC	120	10%
KPS	120	10%
CPS	500	5%
KPCS	100	8%

With probability of $p_m \approx 10^{-7}/4$ per cell per generation, healthy cells will be subject to an activating mutation in a single allele of KRAS. Similarly, we estimate the probability of loss of function mutations in the second copy of CDKN2A (C), TP53 (P), or SMAD4 (S) to be $10^{-7}/4$ per cell per generation. For simplicity, it is assumed that loss of the first copy of these tumor suppressors has no effect on cell fitness. Therefore, healthy N cells are converted with the probability p leading to K , P , C , or S mutant cells, as shown in Figure 1.

These initiating mutations in key genes, K , C , P , and S , would be expected, in many cases, to lead to oncogene induced senescence. Therefore, the loss from the model of these cells upon mutation is defined by probability p_{d_i} . Otherwise, the mutant cells of K type, as demonstrated in Figure 1, can proliferate and die as K -mutants with probabilities shown in Table 1, but can also give a new mutation of P , C , or S type, resulting in KP , KC , or KS double-mutants, correspondingly. At this and consequent stages after adaptation, the new mutants are believed to avoid oncogene induced senescence. These double-mutants can also proliferate, die, or give a rise to triple-mutant cells, i.e., KPS , KPC , KCP , KCS , etc., as shown in Figure 1.

As a result, the overall number of mutated cells is 64. To continue, it is important to enumerate all cell types. The continuous numbering is introduced starting from a single-mutant cells, as illustrated in Table 2 and Figure 1. Overall, the one-letter cells correspond to numbers from 1 to 4, two-letter cells — from 5 to 16, three-letter cells — from 17 to 40, and four-letter cells — from 41 to 64.

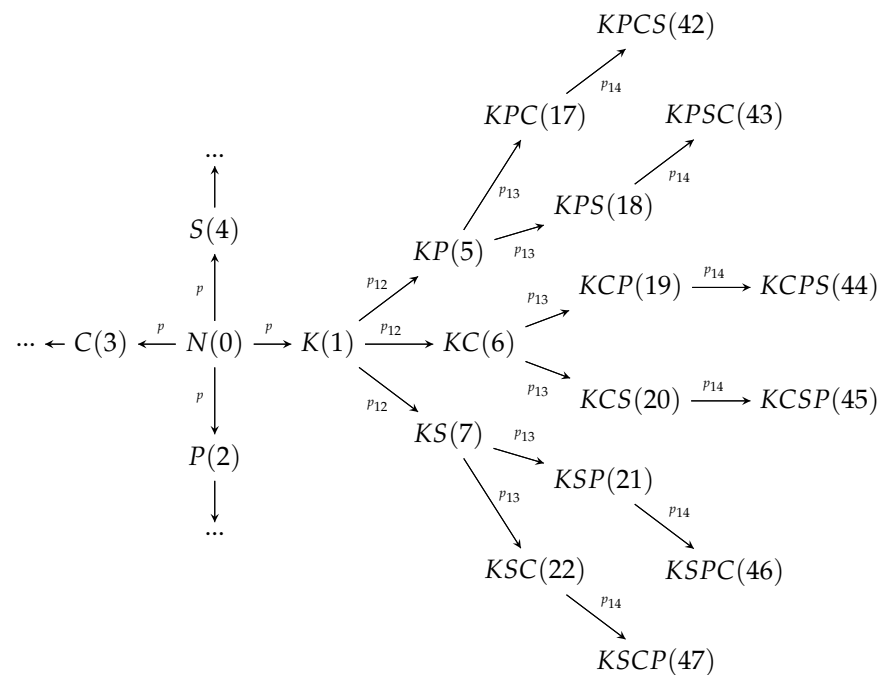


Figure 1. Scheme illustrating the evolution of possible mutations of healthy cell *N*. The branch following the initial mutation *K* is shown in detail. For clarity, the evolutionary schemes evolving from the alternative initial *P*(2), *C*(3), and *S*(4) mutations are not included in the diagram.

Table 2. An illustration of the enumeration rule for the one-letter and two-letter designated types of mutated cells.

Cell type	<i>K</i>	<i>P</i>	<i>C</i>	<i>S</i>	<i>KP</i>	<i>KC</i>	<i>KS</i>	<i>PK</i>
Number	1	2	3	4	5	6	7	8
Cell Type	<i>PC</i>	<i>PS</i>	<i>CK</i>	<i>CP</i>	<i>CS</i>	<i>SK</i>	<i>SP</i>	<i>SC</i>
Number	9	10	11	12	13	14	15	16

Healthy cells mutate into one-letter type with probability $q_0 = p = \frac{1}{4}10^{-7}$. Given the assumptions stated above, the probabilities of one-letter type mutations are $q_1 = pp_1(1 - p_d)$.

Next, we assume that the probabilities of the mutations converting cells with a single mutation into cells carrying two mutations (i.e., one-letter cell types to the two-letter cell types) and the subsequent mutations of these cells into the three-letter and four-letter cell types are identical:

$$p_{m1} = p_1 = \frac{1}{12}, \quad p_{m2} = p_{m3} = p_{m4} = p_2 = \frac{1}{24}.$$

Probabilities of two-letter type mutations are:

$$q_2 = pp_1^2(1 - p_d)^2 \tag{7}$$

Accordingly, three-letter and four-letter:

$$q_3 = pp_1^3(1 - p_d)^3 \tag{8}$$

$$q_4 = pp_1^4(1 - p_d)^4 \tag{9}$$

Unfortunately, data on the probability of instantaneous mortality of p_d species are unknown to us. All subsequent calculations will be made using $p_d = 0.95$.

Fitness rates m_i and death rates d_i in the stated order of cell type enumeration are presented in Figure 2. Based on the data in Table 1, we construct a matrix M that defines the fitness landscape of species. Let us take 1200 days as a unit of fitness (doubling time of healthy cells). All other indicators of the fitness of cell species are calculated by the ratio of the value of 1200 to the corresponding doubling time of the population of each particular species.

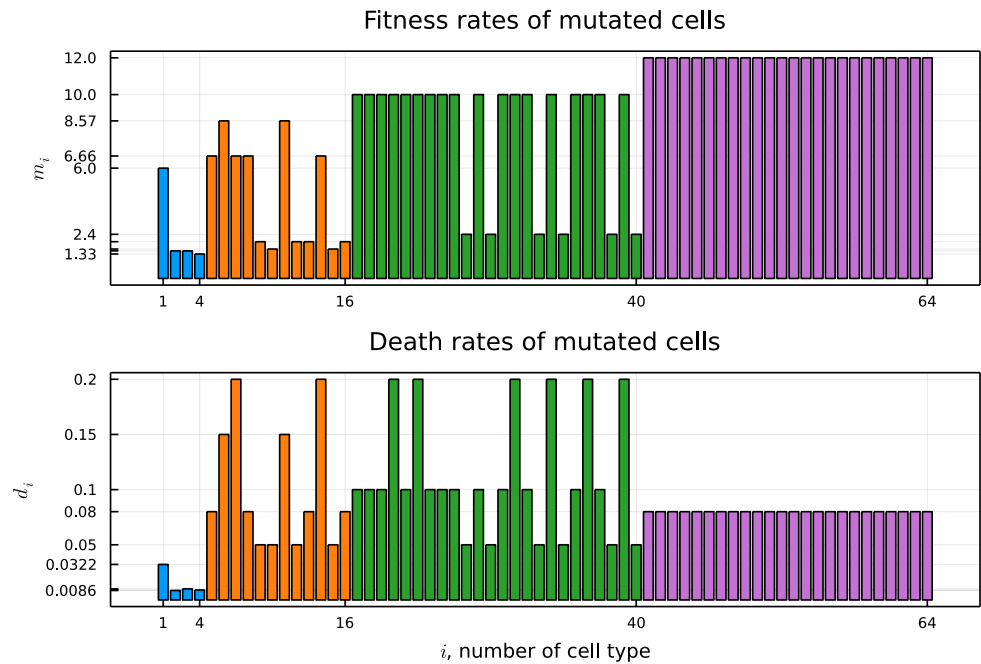


Figure 2. Fitness rates m_i and death rates d_i of mutated cells. Colors correspond to one-letter (blue), two-letter (orange), three-letter (green), and four-letter (magenta) mutations.

3. Model Calibration for Cancer and Precancerous Cell Dynamics

To proceed with the equations of the model, we note that the abundance of nutrients in the pancreas facilitates favorable conditions for healthy, cancerous, and precancerous cells. Until the very latest stages of the disease, the number of healthy pancreatic cells is in vast excess over the number of cancer cells. Therefore, we assume that the number of healthy cells remains constant and the system of equations stated below describes only growth dynamics for cancerous and precancerous cells.

Let \hat{S} be the upper limit of all cells in the pancreas, $S_c(t)$ —number of cancerous and precancerous cells at time $t \geq 0$, $S_c(0) = 0$.

The supply of cells with nutrients is described by function $\psi(t)$, $t \geq 0$, which is the solution to the equation

$$\frac{d\psi(t)}{dt} = r\psi(t) \left(1 - \frac{\psi(t)}{K} \right), \quad \psi(0) = 10^{-5}, \tag{10}$$

where $K = 0.18$ (scaled with respect to the maximal value 1), and $r = 0.00075 \text{ day}^{-1}$.

The system of equations governing the population dynamics of the number of cancerous and precancerous cells is given by

$$\frac{dv_i(t)}{dt} = (\psi(t) - S_c(t)) (\hat{S}(QMv(t))_i + \gamma_i) - d_i v_i(t), \quad v_i(0) = 0, \quad i = 1, \dots, 64. \tag{11}$$

Here $v_i(t)$ is the frequency of the i th cell type relative to \hat{S} , M —diagonal matrix of the fitness landscape $M = \text{diag}(m_1, m_2, \dots, m_{64})$, d_i — the corresponding death rates. The constants γ_i^c ($i = 1, 2, \dots, 64$) characterize the effect of symbiosis between healthy cells

and cancerous and precancerous cells of type i . The numerical values of constants γ_i^c are given in Table 3.

Let q_{ij} are elements of matrix Q , then we have

$$(QMv(t))_i = \sum_{j=1}^{64} q_{ij}m_jv_j(t), \quad i = 1, 2, \dots, 64. \tag{12}$$

Equation (10) implies that the average fitness of the system is given by

$$f(t) = (\psi(t) - S_c(t))^{-1} \tag{13}$$

Table 3. Estimates of the effect of symbiosis between healthy cells and cancerous and precancerous cells of type i .

Mutation type, i	K	P	C	S	KC	KS	KP		
Symbiosis, γ_i^c (10^5)	4	1	1	2	20	24	24		
Mutation type, i	PS	CP	CS	KCS	KPC	KPS	CPS	$KPCS$	
Symbiosis, γ_i^c (10^5)	33	32	32	20	20	20	36	20	

The tumor cells expressing non-self antigens are eliminated by antitumor immune responses mediated by CD8+ T cells (CTL) [23]. However, during cancer progression, CTLs loss their function and acquire an exhaustion state due to immunosuppression within the tumor micro-environment [23–25]. The system of equations accounting for interactions between cancerous and stromal cells and the effect of cancer antigen-induced CD8 T cell response $T(t)$ leads to the model system of ODEs presented below:

$$\begin{aligned} \frac{dv_i(t)}{dt} = & (\psi(t) - S_c(t))(\widehat{S}(QMv(t))_i + \gamma_i^c) - d_i v_i(t) - \\ & - \frac{\gamma_i v_i(t) T(t) \widehat{T}}{K_T + \beta(\widehat{S} S_c(t))^2 + \widehat{T} \cdot T(t)}; \quad v_i(0) = 0, \quad i = 1, 2, \dots, 64. \end{aligned} \tag{14}$$

The last term in the above equation describes the T-cell mediated elimination of cancer cells depending on the functional state of the tumor-specific T cells.

The equation for cancer-specific CD8 T cells takes into account their homeostatic turnover, the cancer-antigens induction of their clonal expansion, and the functional exhaustion taking place when the number of cancer cells increases above a certain threshold.

$$\frac{dT(t)}{dt} = \frac{T^*}{\widehat{T}} + b \frac{\widehat{S} \cdot S_c(t) T(t)}{\omega + \widehat{S}^2 (S_c(t))^2} - d_T T(t), \quad T(0) = 0.3 \tag{15}$$

Hence, it is considered that positive and negative regulations determine the strength of the immune response. For a low or medium abundance of cancer cells, the antiviral immune response is stimulated (the numerator term). However, at high density of cancer cells it gets down-regulated (the denominator term). In particular, for high tumor cell density, the down-regulation of T cell activity takes place (known as functional exhaustion). The description follows the framework previously suggested for virus infections [26,27].

If the we take into account the immune cell-mediated elimination of the cancer cells, then the fitness of the system is defined by

$$f_{im}(t) = f(t) \frac{1}{1 + \frac{C(t)}{D(t)}}. \tag{16}$$

Here the functions $C(\cdot)$, $D(\cdot)$ are given by

$$C(t) = \frac{\hat{T} \cdot T(t) \cdot \sum_{i=1}^{64} \gamma_i v_i(t)}{K_T + \beta(\hat{S} \cdot S_c(t))^2 + \hat{T} \cdot T(t)}, \tag{17}$$

$$D(t) = \sum_{i=1}^{64} d_i v_i(t), \tag{18}$$

and $f(t)$ is the fitness of the system without the impact of the immune system.

Here, $\hat{T} = 2.5 \cdot 10^5$ cells/mL refers to the homeostatic level of tumor-antigen-specific CTLs, $K_T = 10^3$ cells/mL estimates the CTL density for a half-maximal elimination rate of tumor cells, $T^* = 10^3$ cells/mL/day is the homeostatic supply, $d_T = 0.01$ (1/day) is the CTL death rate coefficient, $\beta = 10^{-11}$ (cells/mL)², $b = 10$ day⁻¹, $\omega = 10^7$ (cells/mL)², stand for the down-regulation of the CTL effector function, the clonal proliferation rate of CTLs, and the threshold for cancer cell abundance inducing functional exhaustion in CTLs. For simulations, we used a rescaled value of CTL with respect to their homeostatic abundance \hat{T} .

The software implementation of the model is written in Python version 3.8.8 using jupyter-notebook version 6.3.0. To solve the system of differential equations, the odeint() function from the `scipy.integrate` module was used. The error of this method for each value of the function y_i is equal to:

$$\|e_i\| \leq 1.5 \cdot 10^{-8} \cdot |y_i| + 1.5 \cdot 10^{-8} \tag{19}$$

Graphs were built with a step of 0.1.

4. Computational Experiments

Figure 3 shows the results of numerical calculations of the system without taking into account the interaction with the cells of the immune system. It predicts the evolution of the abundance of the mutants determined by the differences in their fitness values. Cells bearing one mutation appear earlier and have larger population size than that of the two-, three-, and four-mutation cells by a factor of ten.

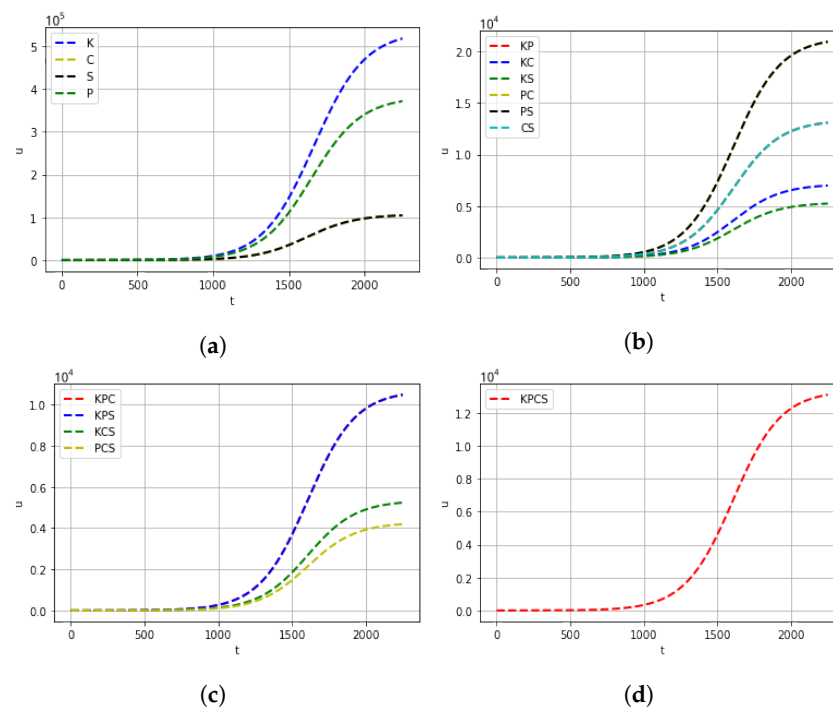
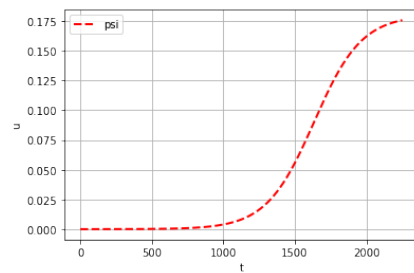


Figure 3. Cont.



(e)

Figure 3. Dynamics of the populations of cancerous and precancerous cells without taking into account the effects of immune cells. The x -axis is the time in days. The y -axis is the number of (quasispecies) mutated pancreatic cells. There are: (a) single mutation cells, (b) two mutation cells, (c) three mutation cells, (d) KPCS cells bearing four mutations, (e) dynamics of nutrients intake.

Figure 4 shows the results of experiments taking into account the interaction of cancer cells with the effector CD8+ T cells of the immune system. The following graphs show the change in the total number of cancer cells under the influence of cells of the immune system. The CTL-mediated elimination of cancer cells slows down the emergence of the single- and double-mutation cells. However, the CTL response fails to control the emergence and abundance of tumor cells with three and four mutations.

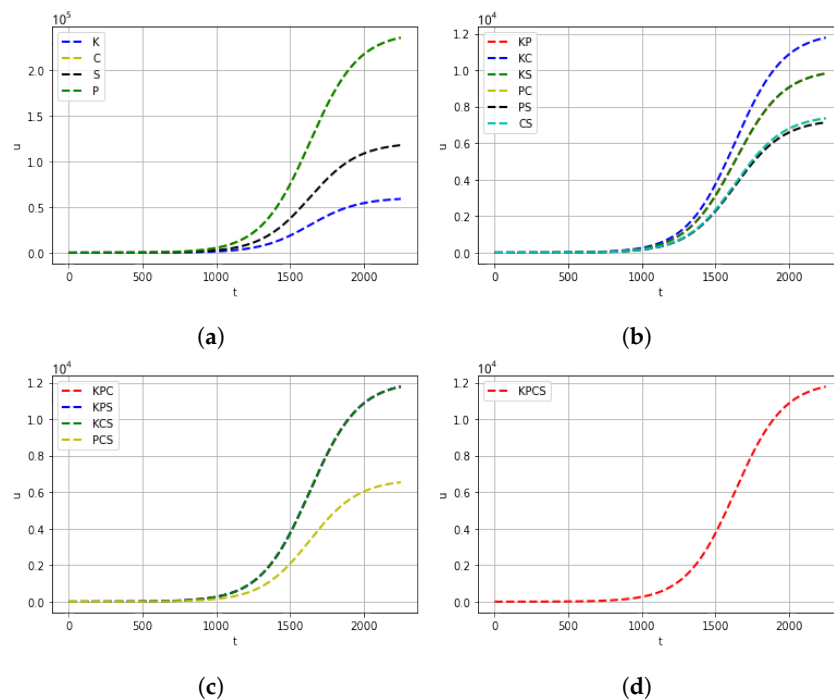


Figure 4. Dynamics of the populations of cancerous and precancerous cells, taking into account the impact of effector CTLs of the immune system. (a) One-mutation cells, (b) two-mutation cells, (c) three-mutation cells, (d) KPCS cells.

The dynamics of the CTL response to tumor antigens is depicted in Figure 5. Initially, the appearance of non-self antigens expressed by tumor cells induces the clonal expansion of CTLs. However, when the density of cancer cells reaches a certain threshold, the immune response is down-regulated (days 650), and the CTLs acquire an exhaustion phenotype.

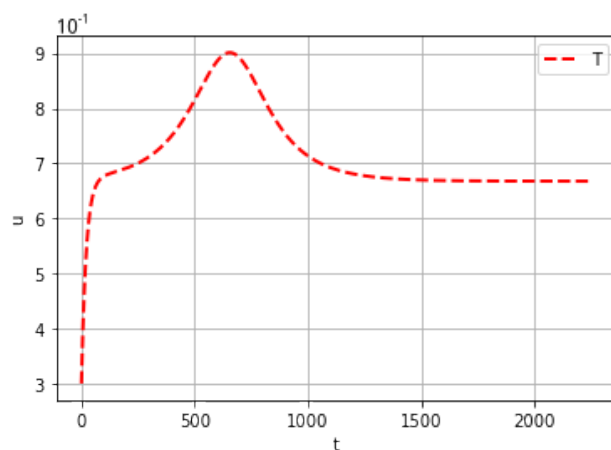


Figure 5. Dynamics of the anti-tumor CTL response. The x -axis is time in days. The y -axis is the relative number of cells on a scale of 10^4 .

Finally, the model can be used to predict the evolution of the mean cancer cell population fitness determining the rate of cancer progression. Figure 6 shows the dynamics of the mean fitness corresponding to uncontrolled growth of cancer cells and the effect of immune control, which delays the emergence of more aggressive cancer quasiespecies.

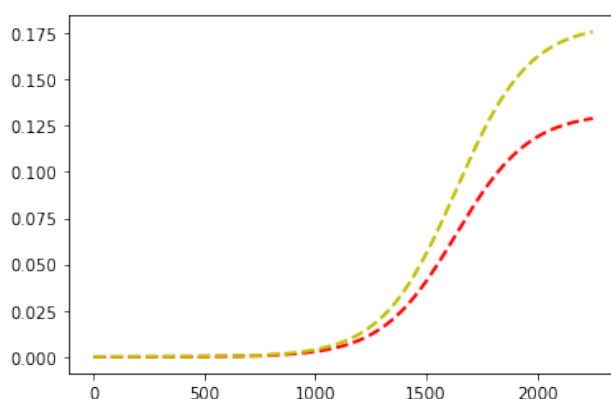


Figure 6. Mean system fitness growth of the cancer cell population without the effect of immune system (yellow line at the top) and taking into account the elimination of cancer cells by effector CTLs (red line at the bottom).

5. Conclusions

In this work, we developed a quantitative mathematical model of the evolutionary dynamics of pancreatic cancer cells. The model describes the emergence of cancer cells bearing different numbers of mutations as evolving quasiespecies systems consisting of 64 subpopulations bearing one, two, three, and four mutations in the most commonly mutated genes in pancreatic cancer, KRAS, CDKN2A, TP53, and SMAD4. In addition, the antitumor CTL response is taken into account and the model consistently reproduces the sequential evolution of cancer cell populations.

In the future, improvements on the model can expand the scope of parameters that contribute to the performance of the model, bringing it closer to the reality of the disease. Further model development should consider the relationship between the number of mutations and the antigenicity of the respective cancer cells, and potentially additional mutations beyond the four considered here. Furthermore, the incorporation of further existing and future data should improve the validity of estimates of the different cell doubling times and mortality rates for specific mutated cell types that are used to calibrate the model dynamics. Finally, there would be benefits to applying stochastic modeling

approaches with the potential to reproduce the unpredictable heterogeneous course of the disease. In summary, our current model and future improvements will provide an analytical tool to examine approaches to the treatment of pancreatic ductal adenocarcinoma, including the chemotherapy, surgery, reinvigoration of exhausted CTLs, and the CAR-T cell therapies [24,25,28,29].

Author Contributions: Conceptualization, A.S.B., N.L., D.Y. and G.B.; methodology, A.S.B., N.L., D.Y. and G.B.; software, M.C.; validation, A.S.B., N.L. and D.Y.; formal analysis, A.S.B. and M.C.; investigation, A.S.B., N.L., M.C., D.Y., D.G., R.S. and G.B.; data curation, N.L.; writing—A.S.B., N.L., M.C., D.Y., D.G., R.S. and G.B.; writing—review and editing, A.S.B., N.L., M.C., D.Y., D.G., R.S. and G.B.; visualization, M.C., D.G. and R.S.; supervision, A.S.B.; funding acquisition, A.S.B. and D.Y. All authors have read and agreed to the published version of the manuscript.

Funding: The reported study was funded by RFBR and the Royal Society of London (RS), project number 21-51-10006. A.B. was supported by the Moscow Center for Fundamental and Applied Mathematics at Lomonosov Moscow State University (agreement with the Ministry of Education and Sciences of the Russian Federation No. 075-219-1621) and D.G., R.S. and G.B. were partly supported by the Moscow Center for Fundamental and Applied Mathematics at INM RAS (agreement with the Ministry of Education and Sciences of the Russian Federation No. 075-15-2022-286).

Data Availability Statement: Not applicable.

Conflicts of Interest: The authors declare no conflict of interest. The funders had no role in the design of the study; in the collection, analyses, or interpretation of data; in the writing of the manuscript, or in the decision to publish the results.

Abbreviations

The following abbreviations are used in this manuscript:

PDAC	Pancreatic ductal adenocarcinoma
CTL	effector CD8+ T lymphocyte
ODE	ordinary differential equation

References

- Kleeff, J.; Korc, M.; Apte, M.; La Vecchia, C.; Johnson, C.D.; Biankin, A.V.; Neale, R.E.; Tempero, M.; Tuveson, D.A.; Hruban, R.H.; et al. Pancreatic cancer. *Nat. Rev. Dis. Prim.* **2016**, *2*, 16022. [[CrossRef](#)]
- Lu, J.; Yu, R.; Liu, R.; Liang, X.; Sun, J.; Zhang, H.; Wu, H.; Zhang, Z.; Shao, Y.W.; Guo, J.; et al. Genetic aberrations in Chinese pancreatic cancer patients and their association with anatomic location and disease outcomes. *Cancer Med.* **2021**, *10*, 933–943. [[CrossRef](#)] [[PubMed](#)]
- Zhou, B.; Xu, J.W.; Cheng, Y.G.; Gao, J.Y.; Hu, S.Y.; Wang, L.; Zhan, H.X. Early detection of pancreatic cancer: Where are we now and where are we going?: Early detection of pancreatic cancer. *Int. J. Cancer* **2017**, *141*, 231–241. [[CrossRef](#)]
- Erkan, M.; Hausmann, S.; Michalski, C.W.; Fingerle, A.A.; Dobritz, M.; Kleeff, J.; Friess, H. The role of stroma in pancreatic cancer: Diagnostic and therapeutic implications. *Nat. Rev. Gastroenterol. Hepatol.* **2012**, *9*, 454–467. [[CrossRef](#)]
- Karamitopoulou, E. Tumour microenvironment of pancreatic cancer: Immune landscape is dictated by molecular and histopathological features. *Br. J. Cancer* **2019**, *121*, 5–14. [[CrossRef](#)] [[PubMed](#)]
- Louzoun, Y.; Xue, C.; Lesinski, G.B.; Friedman, A. A mathematical model for pancreatic cancer growth and treatments. *J. Theor. Biol.* **2014**, *351*, 74–82. [[CrossRef](#)]
- Gaspar, N.J.; Li, L.; Kapoun, A.M.; Medicherla, S.; Reddy, M.; Li, G.; O’Young, G.; Quon, D.; Henson, M.; Damm, D.L.; et al. Inhibition of Transforming Growth Factor β Signaling Reduces Pancreatic Adenocarcinoma Growth and Invasiveness. *Mol. Pharmacol.* **2007**, *72*, 152–161. [[CrossRef](#)]
- Bachem, M.G.; Zhou, S.; Buck, K.; Schneiderhan, W.; Siech, M. Pancreatic stellate cells—role in pancreas cancer. *Langenbeck’s Arch. Surg.* **2008**, *393*, 891–900. [[CrossRef](#)] [[PubMed](#)]
- Mace, T.A.; Ameen, Z.; Collins, A.; Wojcik, S.; Mair, M.; Young, G.S.; Fuchs, J.R.; Eubank, T.D.; Frankel, W.L.; Bekaii-Saab, T.; et al. Pancreatic Cancer-Associated Stellate Cells Promote Differentiation of Myeloid-Derived Suppressor Cells in a STAT3-Dependent Manner. *Cancer Res.* **2013**, *73*, 3007–3018. [[CrossRef](#)]
- Makohon-Moore, A.; Iacobuzio-Donahue, C.A. Pancreatic cancer biology and genetics from an evolutionary perspective. *Nat. Rev. Cancer* **2016**, *16*, 553–565. [[CrossRef](#)] [[PubMed](#)]
- Yachida, S.; Iacobuzio-Donahue, C.A. Evolution and dynamics of pancreatic cancer progression. *Oncogene* **2013**, *32*, 5253–5260. [[CrossRef](#)] [[PubMed](#)]

12. Hayashi, A.; Hong, J.; Iacobuzio-Donahue, C.A. The pancreatic cancer genome revisited. *Nat. Rev. Gastroenterol. Hepatol.* **2021**, *18*, 469–481. [[CrossRef](#)] [[PubMed](#)]
13. Makohon-Moore, A.P.; Zhang, M.; Reiter, J.G.; Bozic, I.; Allen, B.; Kundu, D.; Chatterjee, K.; Wong, F.; Jiao, Y.; Kohutek, Z.A.; et al. Limited heterogeneity of known driver gene mutations among the metastases of individual patients with pancreatic cancer. *Nat. Genet.* **2017**, *49*, 358–366. [[CrossRef](#)] [[PubMed](#)]
14. Yachida, S.; Jones, S.; Bozic, I.; Antal, T.; Leary, R.; Fu, B.; Kamiyama, M.; Hruban, R.H.; Eshleman, J.R.; Nowak, M.A.; et al. Distant metastasis occurs late during the genetic evolution of pancreatic cancer. *Nature* **2010**, *467*, 1114–1117. [[CrossRef](#)] [[PubMed](#)]
15. Notta, F.; Chan-Seng-Yue, M.; Lemire, M.; Li, Y.; Wilson, G.W.; Connor, A.A.; Denroche, R.E.; Liang, S.B.; Brown, A.M.K.; Kim, J.C.; et al. A renewed model of pancreatic cancer evolution based on genomic rearrangement patterns. *Nature* **2016**, *538*, 378–382. [[CrossRef](#)] [[PubMed](#)]
16. Yegorov, I.; Novozhilov, A.S.; Bratus, A.S. Open quasispecies models: Stability, optimization, and distributed extension. *J. Math. Anal. Appl.* **2020**, *481*, 123477. [[CrossRef](#)]
17. Bratus, A.S.; Hu, C.K.; Safro, M.V.; Novozhilov, A.S. On Diffusive Stability of Eigen’s Quasispecies Model. *J. Dyn. Control Syst.* **2014**, *22*, 1–14. [[CrossRef](#)]
18. Volpert, A.I.; Volpert, V.A. *Travelling Wave Solutions of Parabolic Systems*; Translations of Mathematical Monographs Reprint; American Mathematical Society: Providence, RI, USA, 1994.
19. Perrings, C.; Mooney, H.; Mark, W. *Chapter 1 the Problem of Biological Invasions*; Oxford Academic: Oxford, UK, 2009; pp. 1–16. [[CrossRef](#)]
20. Palencia, J.L.D.; González, J.R.; Rahman, S.U.; Redondo, A.N. Regularity, Asymptotic Solutions and Travelling Waves Analysis in a Porous Medium System to Model the Interaction between Invasive and Invaded Species. *Mathematics* **2022**, *10*, 1186. [[CrossRef](#)]
21. Li, Y.; He, Y.; Peng, J.; Su, Z.; Li, Z.; Zhang, B.; Ma, J.; Zhuo, M.; Zou, D.; Liu, X.; et al. Mutant Kras co-opts a proto-oncogenic enhancer network in inflammation-induced metaplastic progenitor cells to initiate pancreatic cancer. *Nat. Cancer* **2021**, *2*, 49–65. [[CrossRef](#)]
22. Mayerle, J. Pancreatic cancer: Why the cell of origin matters. *Nat. Rev. Gastroenterol. Hepatol.* **2022**, *19*, 279–279. [[CrossRef](#)]
23. Farhood, B.; Najafi, M.; Mortezaee, K. CD8⁺ cytotoxic T lymphocytes in cancer immunotherapy: A review. *J. Cell. Physiol.* **2019**, *234*, 8509–8521. [[CrossRef](#)] [[PubMed](#)]
24. Bruni, D.; Angell, H.K.; Galon, J. The immune contexture and Immunoscore in cancer prognosis and therapeutic efficacy. *Nat. Rev. Cancer* **2020**, *20*, 662–680. [[CrossRef](#)] [[PubMed](#)]
25. Mohamed, A.; Huang, Y.H. Life support for transitory exhausted CTLs. *Trends Immunol.* **2021**, *42*, 1057–1059. [[CrossRef](#)] [[PubMed](#)]
26. Bocharov, G. Modelling the Dynamics of LCMV Infection in Mice: Conventional and Exhaustive CTL Responses. *J. Theor. Biol.* **1998**, *192*, 283–308. [[CrossRef](#)]
27. Baral, S.; Antia, R.; Dixit, N.M. A dynamical motif comprising the interactions between antigens and CD8 T cells may underlie the outcomes of viral infections. *Proc. Natl. Acad. Sci. USA* **2019**, *116*, 17393–17398. [[CrossRef](#)]
28. Takano, S.; Fukasawa, M.; Shindo, H.; Takahashi, E.; Hirose, S.; Fukasawa, Y.; Kawakami, S.; Hayakawa, H.; Kuratomi, N.; Kadokura, M.; et al. Clinical significance of genetic alterations in endoscopically obtained pancreatic cancer specimens. *Cancer Med.* **2021**, *10*, 1264–1274. [[CrossRef](#)]
29. Singhi, A.D.; George, B.; Greenbowe, J.R.; Chung, J.; Suh, J.; Maitra, A.; Klempner, S.J.; Hendifar, A.; Milind, J.M.; Golan, T.; et al. Real-Time Targeted Genome Profile Analysis of Pancreatic Ductal Adenocarcinomas Identifies Genetic Alterations That Might Be Targeted With Existing Drugs or Used as Biomarkers. *Gastroenterology* **2019**, *156*, 2242–2253.e4. [[CrossRef](#)]